Signal and Noise Analysis of an MIMO-SSFA

Frédéric Broydé, *Senior Member, IEEE*, and Evelyne Clavelier, *Senior Member, IEEE*

***Abstract*—This brief describes the influences of the source and load impedance matrices on the main small-signal and noise characteristics of a multiple-input-port and multiple-output-port (MIPMOP) device. Expressions for the noise figures of an MIPMOP device are provided in the impedance and admittance representations. We define the natural noise figures as the noise figures evaluated in the case where the multiport source behaves like a noisy passive network at the temperature T_0. This theory is applied to a multiple-input and multiple-output series–series feedback amplifier (MIMO-SSFA), some characteristics of which are computed and measured.**

***Index Terms*—Amplifier noise, amplifiers, feedback circuits, low-noise amplifier (LNA), noise figure, multiple-input and multiple-output (MIMO) systems.**

I. Introduction

THE multiple-input and multiple-output series–series feedback amplifier (MIMO-SSFA), as shown in Fig. 1, may be used in applications such as a transmitting circuit for electrical links [1] or a low-noise amplifier (LNA) for wireless receivers [2], [3]. Used as a transmitting circuit for a multiconductor interconnection connected to a matched termination, an MIMO-SSFA may provide reduced crosstalk. Used as a multiport LNA for a wireless receiver connected to several antennas (e.g., in an MIMO radio system), an MIMO-SSFA may provide Hermitian matching. Elements of the small-signal theory of the MIMO-SSFA were presented in [4], but the influence of the source and load on the signals and the noise characteristics were not analyzed.

Section II addresses the effect of the source and load impedance matrices on the matrices characterizing a linear multiple-input-port and multiple-output-port (MIPMOP) device inserted between an n-port source and an m-port load. These results are applicable to an MIMO-SSFA, and they allow us to compute parameters that may be measured with conventional instruments having uncoupled 50-Ω input/output ports.

Section III covers the characterization, at a given frequency f, of the noise performances of a linear MIPMOP device. The two-port case $n = m = 1$ has been covered in detail in the literature [5], [6], and Haus and Adler presented many results that are applicable to MIPMOP devices [7]. However, they stopped short of defining and discussing an adequate figure of merit, since their original motivation was the systematic description and optimization of the noise performances of a two-port linear amplifier. Recently, Randa [8] has introduced a definition of the noise figures of an MIPMOP device and expressed it using the scattering representation of the device. This formalism is adequate for RF measurements of differential LNAs and has been used by other authors [9]. We provide formulas for computing the noise figures in the impedance or admittance representations, which are more suited for circuit design. We also introduce the definition of "natural noise figures."

Section III covers the design of a validation prototype and the measured gains and input impedances. Section IV covers the natural noise figures of the prototype.

Manuscript received October 5, 2008; revised February 13, 2009. Current version published June 17, 2009. This paper was recommended by Associate Editor A. I. Karsilayan.

The authors are with Excem, 78580 Maule, France (e-mail: fredbroyde@eurexcem.com; eclavelier@eurexcem.com).

Color versions of one or more of the figures in this paper are available online at http://ieeexplore.ieee.org.

Digital Object Identifier 10.1109/TCSII.2009.2020933

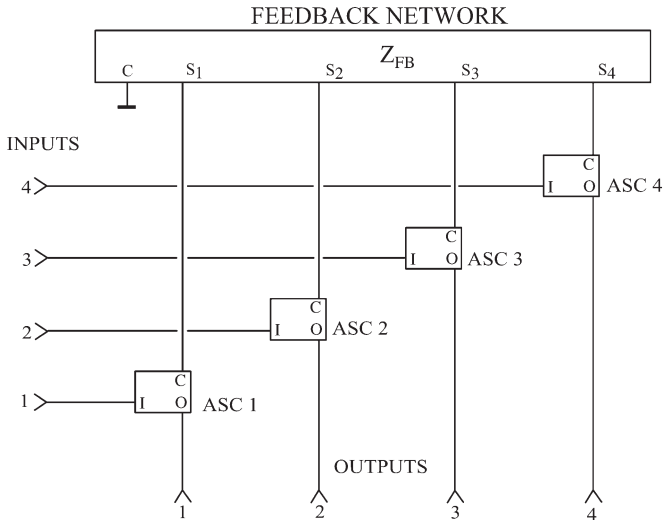

Fig. 1. MIMO-SSFA having four inputs and four outputs, comprising a feedback network (FB) and four ASCs.

II. Influence of the Source and the Load

We number the input and output ports of an MIPMOP device from 1 to n and from 1 to m, respectively. We define the input current i_{Ij} flowing into the positive terminal of port j; the input voltage v_{Ij} between the positive terminal of port j and the negative terminal of port j; the column vector $\mathbf{I}_I$ of the input currents $i_{I1}, \ldots, i_{In}$; and the column vector $\mathbf{V}_I$ of the input voltages $v_{I1}, \ldots, v_{In}$. We also define the output current i_{Ok} flowing into the positive terminal of port k; the output voltage v_{Ok} between the positive terminal of port k and the negative terminal of port k; the column vector $\mathbf{I}_O$ of the output currents $i_{O1}, \ldots, i_{Om}$; and the column vector $\mathbf{V}_O$ of the output voltages $v_{O1}, \ldots, v_{Om}$. If we assume that the MIPMOP device is linear, it is characterized in the frequency domain by [4]

$$\mathbf{I}_I = \mathbf{Y}_I \mathbf{V}_I + \mathbf{Y}_R \mathbf{V}_O \tag{1}$$

$$\mathbf{I}_O = \mathbf{Y}_T \mathbf{V}_I + \mathbf{Y}_O \mathbf{V}_O \tag{2}$$

where $\mathbf{Y}_I$ is a square $n \times n$ matrix, $\mathbf{Y}_O$ is a square $m \times m$ matrix, $\mathbf{Y}_R$ is an $n \times m$ matrix, and $\mathbf{Y}_T$ is an $m \times n$ matrix.

The MIPMOP device may also be considered as an $(n+m)$-port characterized by a single admittance matrix $\mathbf{Y}$ of size $(n+m)\times(n+m)$ such that

$$\begin{pmatrix}\mathbf{I}_I\\ \mathbf{I}_O\end{pmatrix}=\mathbf{Y}\begin{pmatrix}\mathbf{V}_I\\ \mathbf{V}_O\end{pmatrix},\qquad \mathbf{Y}=\begin{pmatrix}\mathbf{Y}_I & \mathbf{Y}_R\\ \mathbf{Y}_T & \mathbf{Y}_O\end{pmatrix}. \tag{3}$$

When the output ports of the MIPMOP device are connected to an m-port load presenting the impedance matrix $\mathbf{Z}_L$ of size $m\times m$, the input ports of the MIPMOP device present an admittance matrix $\mathbf{Y}_{LI}$, which is referred to as the loaded input admittance matrix. The loaded input admittance matrix is given by

$$\begin{aligned}\mathbf{Y}_{LI}&=\mathbf{Y}_I-\mathbf{Y}_R(\mathbf{1}_m+\mathbf{Z}_L\mathbf{Y}_O)^{-1}\mathbf{Z}_L\mathbf{Y}_T\\ &=\mathbf{Y}_I-\mathbf{Y}_R\mathbf{Z}_L(\mathbf{1}_m+\mathbf{Y}_O\mathbf{Z}_L)^{-1}\mathbf{Y}_T\end{aligned} \tag{4}$$

where $\mathbf{1}_m$ is the identity matrix of size $m\times m$. In the same way, when the input ports of an MIPMOP device are connected to an n-port source presenting the impedance matrix $\mathbf{Z}_S$ of size $n\times n$, the output ports of the MIPMOP device present an admittance matrix $\mathbf{Y}_{LO}$, which we will call the loaded output admittance matrix. The loaded output admittance matrix is given by

$$\begin{aligned}\mathbf{Y}_{LO}&=\mathbf{Y}_O-\mathbf{Y}_T(\mathbf{1}_n+\mathbf{Z}_S\mathbf{Y}_I)^{-1}\mathbf{Z}_S\mathbf{Y}_R\\ &=\mathbf{Y}_O-\mathbf{Y}_T\mathbf{Z}_S(\mathbf{1}_n+\mathbf{Y}_I\mathbf{Z}_S)^{-1}\mathbf{Y}_R.\end{aligned} \tag{5}$$

The voltage gain matrix $\mathbf{G}_V$ that is defined by $\mathbf{V}_O=\mathbf{G}_V\mathbf{V}_I$ is given by

$$\begin{aligned}\mathbf{G}_V&=-(\mathbf{1}_n+\mathbf{Z}_L\mathbf{Y}_O)^{-1}\mathbf{Z}_L\mathbf{Y}_T\\ &=-\mathbf{Z}_L(\mathbf{1}_n+\mathbf{Y}_O\mathbf{Z}_L)^{-1}\mathbf{Y}_T.\end{aligned} \tag{6}$$

If we apply these general results to an MIMO-SSFA, we have $n=m$, and the negative terminals of all ports are grounded. Using a vector network analyzer, it is possible to measure $\mathbf{Y}_{LI}$ for a given $\mathbf{Z}_L$ and $\mathbf{Y}_{LO}$ for a given $\mathbf{Z}_S$. In practice, however, only some direct impedance measurements are possible: n *in situ* input impedances and n *in situ* output impedances. We define each *in situ* input impedance or *in situ* output impedance as the impedance seen by a single-port source connected to any one of the inputs or outputs of the MIMO-SSFA, respectively, when the other inputs and outputs are connected to 50-Ω resistors. If $\mathbf{Y}_{LI}$ is determined for $\mathbf{Z}_L=50\times\mathbf{1}_n\ \Omega$, one of the *in situ* input impedances is, for instance, given by

$$z_{\mathrm{in}1}=\left[\left(\mathbf{Y}_{LI}+\frac{1}{50\,\Omega}\mathrm{diag}_n(0,1,\ldots,1)\right)^{-1}\begin{pmatrix}1\\0\\\vdots\\0\end{pmatrix}\right]_1 \tag{7}$$

where $\mathrm{diag}_n(a_1,\ldots,a_n)$ is the diagonal matrix of order n having the diagonal entries a_i, and where $[\mathbf{u}]_i$ is the ith entry of the vector $\mathbf{u}$. If $\mathbf{Y}_{LO}$ is determined for $\mathbf{Z}_S=50\times\mathbf{1}_n\ \Omega$, one of the *in situ* output impedances is, for instance, given by

$$z_{\mathrm{out}1}=\left[\left(\mathbf{Y}_{LO}+\frac{1}{50\,\Omega}\mathrm{diag}_n(0,1,\ldots,1)\right)^{-1}\begin{pmatrix}1\\0\\\vdots\\0\end{pmatrix}\right]_1. \tag{8}$$

Clearly, the n *in situ* input impedances must be close to 50 Ω if we want to avoid reflections in 50-Ω coaxial cables used to connect one of the input ports of the MIMO-SSFA to a source of signal, when all other inputs ports and the output ports are connected to 50-Ω terminations.

We define each *in situ* voltage gain vector as $1/x$ times the column vector of the output voltages, when one of the inputs is connected to a 50-Ω generator delivering x volts according to the high-frequency convention (i.e., an open-circuit voltage of $2x$ volts), the other inputs and all outputs being connected to 50-Ω resistors. If $\mathbf{Y}_{LI}$ is determined for $\mathbf{Z}_L=50\times\mathbf{1}_n\ \Omega$, and if $\mathbf{Z}_S=50\times\mathbf{1}_n\ \Omega$, one of the n *in situ* voltage gain vectors is, for instance, given by

$$\mathbf{G}_{\mathrm{VIS}1}=\mathbf{G}_V\left(\mathbf{Y}_{LI}+\mathbf{Z}_S^{-1}\right)^{-1}\begin{pmatrix}2/50\ \Omega\\0\\\vdots\\0\end{pmatrix}. \tag{9}$$

The square of the absolute value of each entry of the *in situ* voltage gain vector is the insertion power gain (IPG) between the corresponding input and the corresponding output, which can easily be directly measured.

III. Noise Figures of an MIPMOP Device

We shall use root-mean-square values and $\mathbf{X}^*$ to denote the Hermitian adjoint of a matrix $\mathbf{X}$. In a small bandwidth Δf around a given frequency f, we define the column vector $\mathbf{I}_{\mathrm{IN}}$ of the input noise currents $i_{\mathrm{IN}1},\ldots,i_{\mathrm{IN}n}$ flowing into the positive terminal of the input ports of the MIPMOP device and the column vector $\mathbf{V}_{\mathrm{IN}}$ of the input noise voltages $v_{\mathrm{IN}1},\ldots,v_{\mathrm{IN}n}$ between the positive and negative terminals of the input ports. We use $\mathbf{I}_{\mathrm{SCIN}}$ and $\mathbf{V}_{\mathrm{OCIN}}$ to denote the column vectors of the short-circuit input noise currents $i_{\mathrm{SCIN}1},\ldots,i_{\mathrm{SCIN}n}$ and of the open-circuit input noise voltages $v_{\mathrm{OCIN}1},\ldots,v_{\mathrm{OCIN}n}$, respectively. We also define the column vector $\mathbf{I}_{\mathrm{ON}}$ of the output noise currents $i_{\mathrm{ON}1},\ldots,i_{\mathrm{ON}m}$ flowing into the positive terminal of the output ports and the column vector $\mathbf{V}_{\mathrm{ON}}$ of the output noise voltages $v_{\mathrm{ON}1},\ldots,v_{\mathrm{ON}m}$ between the positive and negative terminals of the output ports. We use $\mathbf{I}_{\mathrm{SCON}}$ and $\mathbf{V}_{\mathrm{OCON}}$ to denote the column vectors of the short-circuit output noise currents $i_{\mathrm{SCON}1},\ldots,i_{\mathrm{SCON}m}$ and of the open-circuit output noise voltages $v_{\mathrm{OCON}1},\ldots,v_{\mathrm{OCON}m}$, respectively. Let us write

$$\mathbf{V}_N=\begin{pmatrix}\mathbf{V}_{\mathrm{IN}}\\ \mathbf{V}_{\mathrm{ON}}\end{pmatrix}\quad \mathbf{V}_{\mathrm{OCN}}=\begin{pmatrix}\mathbf{V}_{\mathrm{OCIN}}\\ \mathbf{V}_{\mathrm{OCON}}\end{pmatrix} \tag{10}$$

$$\mathbf{I}_N=\begin{pmatrix}\mathbf{I}_{\mathrm{IN}}\\ \mathbf{I}_{\mathrm{ON}}\end{pmatrix}\qquad \mathbf{I}_{\mathrm{SCN}}=\begin{pmatrix}\mathbf{I}_{\mathrm{SCIN}}\\ \mathbf{I}_{\mathrm{SCON}}\end{pmatrix}. \tag{11}$$

For the case $n=m=2$, we obtain the equivalent circuit in the impedance representation shown in Fig. 2(a), consisting of $n+m=4$ voltage sources and one noiseless $(n+m)$-port. Such an equivalent circuit corresponds to

$$\mathbf{V}_N=\mathbf{Z}\mathbf{I}_n+\mathbf{V}_{\mathrm{OCN}} \tag{12}$$

where $\mathbf{Z}=\mathbf{Y}^{-1}$, $\mathbf{Y}$ being defined by (3). Alternatively, we obtain the equivalent circuit in the admittance representation shown in Fig. 2(b), consisting of $n+m=4$ current

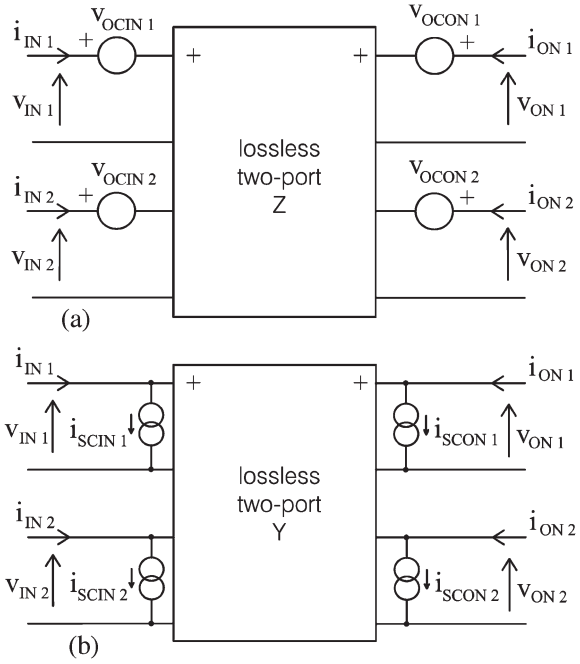

Fig. 2. Equivalent circuit for a noisy MIPMOP device.

sources and one noiseless $(n+m)$-port. This equivalent circuit corresponds to

$$\mathbf{I}_N = \mathbf{Y}\mathbf{V}_N + \mathbf{I}_{\mathrm{SCN}}. \tag{13}$$

We obtain

$$\begin{cases} \mathbf{V}_{\mathrm{OCN}} = -\mathbf{Z}\mathbf{I}_{\mathrm{SCN}} \\ \mathbf{I}_{\mathrm{SCN}} = -\mathbf{Y}\mathbf{V}_{\mathrm{OCN}}. \end{cases} \tag{14}$$

The second-order statistics of the noise produced by the MIPMOP device is determined by the covariance matrix of the open-circuit voltages $\langle \mathbf{V}_{\mathrm{OCN}}\mathbf{V}^*_{\mathrm{OCN}} \rangle$ or, equivalently, by the covariance matrix of the short-circuit currents $\langle \mathbf{I}_{\mathrm{SCN}}\mathbf{I}^*_{\mathrm{SCN}} \rangle$, where the brackets $\langle\ \rangle$ indicate an average over an ensemble of noise processes. The covariance matrices are related by

$$\begin{cases} \langle \mathbf{V}_{\mathrm{OCN}}\mathbf{V}^*_{\mathrm{OCN}} \rangle = \mathbf{Z} \langle \mathbf{I}_{\mathrm{SCN}}\mathbf{I}^*_{\mathrm{SCN}} \rangle \mathbf{Z}^* \\ \langle \mathbf{I}_{\mathrm{SCN}}\mathbf{I}^*_{\mathrm{SCN}} \rangle = \mathbf{Y} \langle \mathbf{V}_{\mathrm{OCN}}\mathbf{V}^*_{\mathrm{OCN}} \rangle \mathbf{Y}^*. \end{cases} \tag{15}$$

In the definition of the noise figure of a two-port, the spectral density of the available power of the noise delivered by the source is kT_0, where k is the Boltzmann's constant, and $T_0 = 290$ K. In the case of devices having several input ports, we have to consider that the noises delivered by the different ports of the n-port source may be correlated and may have different noise temperatures. We shall use the following definition.

Definition 1: If α is an integer such that $1 \leq \alpha \leq m$, the noise figure F_α of the MIPMOP device for the output α is the ratio of the self-power spectral density $\mathrm{Re}(\langle v_{\mathrm{ON}\alpha}\overline{i_{\mathrm{ON}\alpha}} \rangle)/\Delta f$ at the output α to the portion of this self-power spectral density that is due to the input noise, evaluated for the case where (a) the available power spectral density of the n-port source is nkT_0 and (b) the available power of the noise delivered by the load is zero.

This definition of the m spot noise figures is identical to the definition introduced by Randa [8] using the scattering representation, except that the condition (a) is not required in his definition. We use it because it guaranties that our general definition becomes the usual definition in the two-port case.

Let us first assume that the impedance matrix of the source is $\mathbf{Z}_S$, that the column vector of the open-circuit noise voltages produced by the source is $\mathbf{E}_{\mathrm{SN}}$, and that the impedance matrix of the (noiseless) load is $\mathbf{Z}_L$. Clearly, we have

$$\mathbf{V}_N = \begin{pmatrix} \mathbf{E}_{\mathrm{SN}} \\ \mathbf{0}_{m1} \end{pmatrix} - \mathbf{Z}_{\mathrm{SL}}\mathbf{I}_n, \qquad \mathbf{Z}_{\mathrm{SL}} = \begin{pmatrix} \mathbf{Z}_S & \mathbf{0}_{nm} \\ \mathbf{0}_{mn} & \mathbf{Z}_L \end{pmatrix} \tag{16}$$

where $\mathbf{0}_{pq}$ is used to denote the null matrix of size $p \times q$.

In the impedance representation, it is possible to prove that F_α is given by (17), shown at the bottom of the page, where $[\mathbf{X}]_{ij}$ is the entry of row i and column j of the matrix $\mathbf{X}$, and where

$$\mathbf{Z}_{\mathrm{HL}} = \begin{pmatrix} \mathbf{0}_{nn} & \mathbf{0}_{nm} \\ \mathbf{0}_{mn} & \mathbf{Z}_L \end{pmatrix} \tag{18}$$

Alternatively, we can use $\mathbf{Y}_S$ to denote the admittance matrix of the source, $\mathbf{J}_{\mathrm{SN}}$ to denote the column vector of the short-circuit noise currents produced by the source, and $\mathbf{Y}_L$ to denote the admittance matrix of the (noiseless) load. Here, we have

$$\mathbf{I}_N = \begin{pmatrix} \mathbf{J}_{\mathrm{SN}} \\ \mathbf{0}_{m1} \end{pmatrix} - \mathbf{Y}_{\mathrm{SL}}\mathbf{V}_n, \qquad \mathbf{Y}_{\mathrm{SL}} = \begin{pmatrix} \mathbf{Y}_S & \mathbf{0}_{nm} \\ \mathbf{0}_{mn} & \mathbf{Y}_L \end{pmatrix}. \tag{19}$$

In the admittance representation, it is possible to prove that F_α is given by (20), shown at the bottom of the page, where

$$\mathbf{Y}_{\mathrm{HL}} = \begin{pmatrix} \mathbf{0}_{nn} & \mathbf{0}_{nm} \\ \mathbf{0}_{mn} & \mathbf{Y}_L \end{pmatrix}. \tag{21}$$

$$F_\alpha = 1 + \frac{\mathrm{Re}\left(\left[\mathbf{Z}_{\mathrm{HL}}(\mathbf{Z}+\mathbf{Z}_{\mathrm{SL}})^{-1} \langle \mathbf{V}_{\mathrm{OCN}}\mathbf{V}^*_{\mathrm{OCN}} \rangle (\mathbf{Z}+\mathbf{Z}_{\mathrm{SL}})^{-1*} \right]_{n+\alpha\ n+\alpha} \right)}{\mathrm{Re}\left(\left[\mathbf{Z}_{\mathrm{HL}}(\mathbf{Z}+\mathbf{Z}_{\mathrm{SL}})^{-1} \begin{pmatrix} \langle \mathbf{E}_{\mathrm{SN}}\mathbf{E}^*_{\mathrm{SN}} \rangle & \mathbf{0}_{nm} \\ \mathbf{0}_{mn} & \mathbf{0}_{mm} \end{pmatrix} (\mathbf{Z}+\mathbf{Z}_{\mathrm{SL}})^{-1*} \right]_{n+\alpha\ n+\alpha} \right)} \tag{17}$$

$$F_\alpha = 1 + \frac{\mathrm{Re}\left(\left[(\mathbf{Y}+\mathbf{Y}_{\mathrm{SL}})^{-1} \langle \mathbf{I}_{\mathrm{SCN}}\mathbf{I}^*_{\mathrm{SCN}} \rangle (\mathbf{Y}+\mathbf{Y}_{\mathrm{SL}})^{-1*}\mathbf{Y}^*_{\mathrm{HL}} \right]_{n+\alpha\ n+\alpha} \right)}{\mathrm{Re}\left(\left[(\mathbf{Y}+\mathbf{Y}_{\mathrm{SL}})^{-1} \begin{pmatrix} \langle \mathbf{J}_{\mathrm{SN}}\mathbf{J}^*_{\mathrm{SN}} \rangle & \mathbf{0}_{nm} \\ \mathbf{0}_{mn} & \mathbf{0}_{mm} \end{pmatrix} (\mathbf{Y}+\mathbf{Y}_{\mathrm{SL}})^{-1*}\mathbf{Y}^*_{\mathrm{HL}} \right]_{n+\alpha\ n+\alpha} \right)} \tag{20}$$

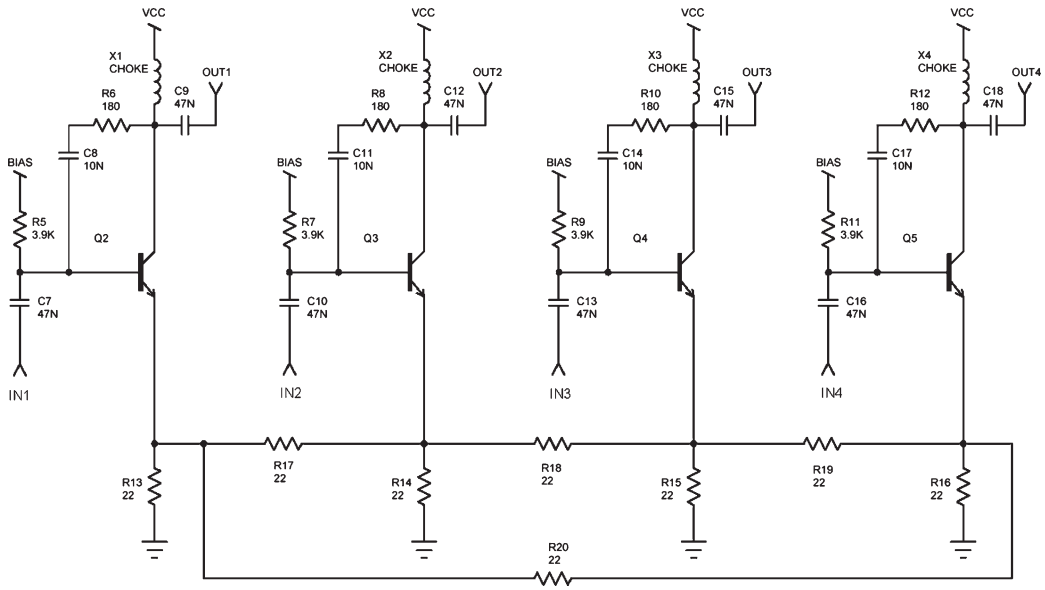

Fig. 3. MIMO-SSFA used for the experimental validation.

It is also possible to show that, if the source produces the noise of a noisy passive network at the temperature T_0, then

$$\langle \mathbf{E}_{\rm SN}\mathbf{E}_{\rm SN}^{*}\rangle = 2kT_0\Delta f\,(\mathbf{Z}_S + \mathbf{Z}_S^{*}) \quad (22)$$

$$\langle \mathbf{J}_{\rm SN}\mathbf{J}_{\rm SN}^{*}\rangle = 2kT_0\Delta f\,(\mathbf{Y}_S + \mathbf{Y}_S^{*})\,. \quad (23)$$

Consequently, in this case, the available power spectral density of the n-port source is nkT_0, and the constraint (a) of the definition of the noise figures of an MIPMOP device is automatically satisfied. This leads us to Definition 2.

Definition 2: The natural noise figures are the noise figures evaluated for the case where the source produces the noise of a noisy passive network at the temperature T_0.

The matrices $\mathbf{Z}_S$ and $\mathbf{Z}_L$ appear in (17) and (20). Examples show that, in general, the noise figure and the natural noise figure depend on $\mathbf{Z}_S$ and $\mathbf{Z}_L$. This is in contrast with the noise figure in the two-port-case, which depends on the source impedance, but not on the load impedance.

The reason for this fundamental difference appears if we consider the special case in which $\mathbf{Z}_S$ and $\mathbf{Z}_L$ are both diagonal. In this case, we may define the noise figure $F_{\alpha\beta}$ between an input β and an output α as the usual noise figure of a two-port, evaluated when all unused inputs and outputs are connected to uncorrelated single-port terminations. In addition, we have

$$\frac{1}{F_\alpha} = \sum_{\beta=1}^{n} \frac{1}{F_{\alpha\beta}}. \quad (24)$$

We see that the two-port used to define $F_{\alpha\beta}$ is modified by any change of a diagonal entry of $\mathbf{Z}_L$ other than the αth, so that such a change modifies $F_{\alpha\beta}$. We are therefore not surprised that the F_α given by (24) depends on $\mathbf{Z}_L$.

IV. Validation Prototype

The validation prototype shown in Fig. 3 has four inputs (i.e., IN1–IN4) and four outputs (i.e., OUT1–OUT4). This MIMO-SSFA is made of discrete components, using an HFA3127B transistor array comprising five transistors. One transistor of the array (Q1, not shown in Fig. 3) is used to obtain a base-biasing voltage producing, in each of the transistors Q2–Q5 shown in Fig. 3, a collector current of 10 mA for VCC $= 5$ V. Each active subcircuit (ASC) comprises a transistor, a shunt–shunt feedback branch (C8, R6), a base-biasing circuit (R5, C7), and a collector-biasing circuit (X1, C9). The circuit element X1 is an elaborate choke coil made of several inductors and resistors. The feedback network producing the series–series feedback is made of eight surface-mounted device resistors (R13–R20).

This MIMO-SSFA is invariant under a circular permutation of the inputs and outputs. Such a structure is typical of a transmitting circuit capable of providing four channels with a low crosstalk in a shielded star-quad cable, which presents a rotational symmetry.

Based on the SPICE parameters provided by the manufacturer, we computed the admittance matrix $\mathbf{Y}_A$ of the ASCs, as defined by [4, eq. (3)], versus frequency. The matrices $\mathbf{Y}_I$, $\mathbf{Y}_O$, $\mathbf{Y}_R$, and $\mathbf{Y}_T$ of the MIMO-SSFA were obtained using

$$\mathbf{Y}_T = y_{A31}\mathbf{1}_n + y_{A32}y_{A21}\mathbf{Z}_{\rm FB}[\mathbf{1}_n - y_{A22}\mathbf{Z}_{\rm FB}]^{-1} \quad (25)$$

$$\mathbf{Y}_O = y_{A33}\mathbf{1}_n + y_{A32}y_{A23}\mathbf{Z}_{\rm FB}[\mathbf{1}_n - y_{A22}\mathbf{Z}_{\rm FB}]^{-1} \quad (26)$$

$$\mathbf{Y}_I = y_{A11}\mathbf{1}_n + y_{A12}y_{A21}\mathbf{Z}_{\rm FB}[\mathbf{1}_n - y_{A22}\mathbf{Z}_{\rm FB}]^{-1} \quad (27)$$

$$\mathbf{Y}_R = y_{A13}\mathbf{1}_n + y_{A12}y_{A23}\mathbf{Z}_{\rm FB}[\mathbf{1}_n - y_{A22}\mathbf{Z}_{\rm FB}]^{-1} \quad (28)$$

where $\mathbf{Z}_{\rm FB}$ is the impedance matrix of the feedback network, and where we use y_{Aij} to denote the entries of $\mathbf{Y}_A$. Thus, we were able to obtain $\mathbf{Y}_{LI}$, $\mathbf{Y}_{LO}$, $\mathbf{G}_V$, $z_{\rm in1}$, $z_{\rm out1}$, and $G_{\rm VIS1}$, as given in (4)–(9), respectively, and we could adjust the shunt–shunt feedback branch and the feedback network to obtain the desired characteristics.

One of the design targets was an *in situ* input impedance close to 50 Ω in the 1- to 100-MHz band. The measured values are $(46 + j6)$ Ω at 30 MHz and $(55 + j15)$ Ω at 100 MHz. Fig. 4 shows the computed IPGs between the input IN1 and the four outputs OUT1–OUT4 (solid curves) and the measured IPGs (dashed curves). Our computation did not include the package and breadboard parasitics, so that the drop of all measured IPGs above 100 MHz is attributable to the stray self-inductances and the mutual inductances in the feedback network. The inaccuracies shown in Fig. 4 in the computed IPGs

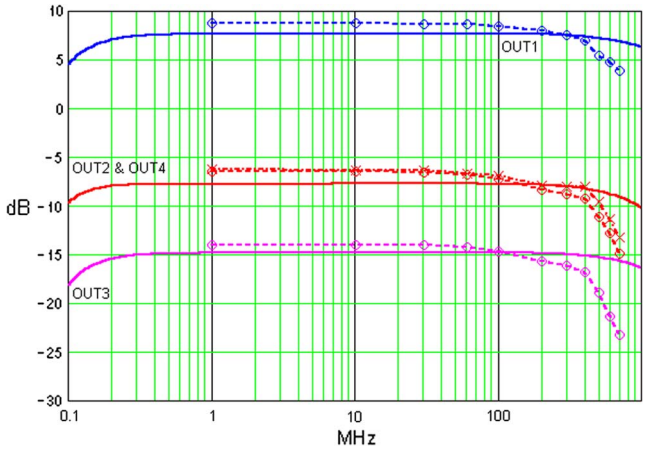

Fig. 4. Computed and measured IPGs.

below 100 MHz (up to 1.4 dB at 10 MHz) are mainly caused by the manufacturer-supplied SPICE model for the transistors. We later disconnected Q1 and characterized it in a common–emitter test circuit. We then defined a new SPICE model, providing a good agreement between the measurement and the simulation for the said test circuit. For the MIMO-SSFA at 10 MHz, the IPGs computed with the new SPICE model were within 0.3 dB of the measured IPGs (8.55 dB for OUT1, −6.55 dB for OUT2, −14.01 dB for OUT3, and −6.37 dB for OUT4).

V. Noise Figures of the Validation Prototype

We also measured the noise figure of Q1 in the said common–emitter configuration for a 50-Ω source impedance: We obtained $F = 2.9$ at 10 MHz. The result was used to adjust the r'_b of the Nielsen's transistor model [10], to which an emitter capacitance was added to obtain an emitter-limited transistor model [11]. Using (15) to obtain the appropriate representation, the covariance matrix of the series or parallel connection of two uncorrelated circuits is clearly obtained as a sum of covariance matrices [12], [13]. In this manner, we successively computed the following:

1) the covariance matrix of the open-circuit voltages $\langle \mathbf{V}_A \mathbf{V}_A^* \rangle$ of the floating three-terminal circuit comprising a transistor and a shunt–shunt feedback branch used in the ASCs, this matrix being given by

$$\langle \mathbf{V}_A \mathbf{V}_A^* \rangle = \begin{pmatrix} \langle V_{A1} \overline{V_{A1}} \rangle & \langle V_{A1} \overline{V_{A2}} \rangle \\ \langle V_{A1} \overline{V_{A2}} \rangle & \langle V_{A2} \overline{V_{A2}} \rangle \end{pmatrix} \tag{29}$$

where the bar denotes complex conjugation;

2) the covariance matrix $\langle \mathbf{V}_B \mathbf{V}_B^* \rangle$ of the open-circuit voltages of the circuit consisting of the four aforementioned floating three-terminal circuits connected in series with the feedback network, using

$$\langle \mathbf{V}_B \mathbf{V}_B^* \rangle = \begin{pmatrix} \langle \mathbf{E}_{\rm FB} \mathbf{E}_{\rm FB}^* \rangle & \langle \mathbf{E}_{\rm FB} \mathbf{E}_{\rm FB}^* \rangle \\ \langle \mathbf{E}_{\rm FB} \mathbf{E}_{\rm FB}^* \rangle & \langle \mathbf{E}_{\rm FB} \mathbf{E}_{\rm FB}^* \rangle \end{pmatrix} + \begin{pmatrix} \langle V_{A1} \overline{V_{A1}} \rangle \mathbf{1}_n & \langle V_{A1} \overline{V_{A2}} \rangle \mathbf{1}_n \\ \langle V_{A1} \overline{V_{A2}} \rangle \mathbf{1}_n & \langle V_{A2} \overline{V_{A2}} \rangle \mathbf{1}_n \end{pmatrix} \tag{30}$$

and the assumption that the feedback network of the MIMO-SSFA behaves as a noisy passive network at the temperature T_0, so that, in line with (22), the covariance matrix of the open-circuit voltages at the terminals of the feedback network is

$$\langle \mathbf{E}_{\rm FB} \mathbf{E}_{\rm FB}^* \rangle = 2kT_0 \Delta f \, (\mathbf{Z}_{\rm FB} + \mathbf{Z}_{\rm FB}^*) \tag{31}$$

3) the matrix $\langle \mathbf{I}_{\rm SCN} \mathbf{I}_{\rm SCN}^* \rangle$ of the MIMO-SSFA, once the biasing circuits are included.

Using (20) and (23), the natural noise figures of the MIMO-SSFA were computed. We found $F_1 = F_2 = F_3 = F_4 = 5.7$ at 10 MHz, for $\mathbf{Z}_S = \mathbf{Z}_L = 50 \times \mathbf{1}_4\ \Omega$.

Using the measured values of F_{11}, F_{12}, F_{13}, and F_{14} and (24), we obtained the natural noise figure $F_1 = 6.0$ at 10 MHz, for $\mathbf{Z}_S = \mathbf{Z}_L = 50 \times \mathbf{1}_4\ \Omega$, which is in good agreement with the computed value.

VI. Conclusion

At the design stage, we have shown how $\mathbf{Z}_S$ and $\mathbf{Z}_L$ may be taken into account to compute $\mathbf{Y}_{LI}$, $\mathbf{Y}_{LO}$, $\mathbf{G}_V$, and the noise figures F_α. We have defined the natural noise figures.

In the case $\mathbf{Z}_S = \mathbf{Z}_L = 50 \times \mathbf{1}_n\ \Omega$, the *in situ* parameters and the noise figures $F_{\alpha\beta}$ may easily be measured with conventional instruments, so that the natural noise figures F_α may be derived.

References

[1] F. Broydé and E. Clavelier, "A simple method for transmission with reduced crosstalk and echo," in *Proc. 13th IEEE ICECS*, Dec. 10–13, 2006, pp. 684–687.

[2] F. Broydé and E. Clavelier, "Taking advantage of mutual coupling in radio-communication systems using a multi-port antenna array," *IEEE Antennas Propag. Mag.*, vol. 49, no. 4, pp. 208–220, Aug. 2007.

[3] F. Broydé and E. Clavelier, "Multiple-input-port and multiple-output-port amplifier for wireless receivers," in *Proc. SAME Forum*, Nice, France, Oct. 3/4, 2007. [Online]. Available: http://www.eurexcem.com

[4] F. Broydé and E. Clavelier, "MIMO series–series feedback amplifiers," *IEEE Trans. Circuits Syst. II, Exp. Briefs*, vol. 54, no. 12, pp. 1037–1041, Dec. 2007.

[5] H. Rothe and W. Dahlke, "Theory of noisy four poles," *Proc. IRE*, vol. 44, no. 6, pp. 811–817, Jun. 1956.

[6] K. Hartmann, "Noise characterization of linear circuits," *IEEE Trans. Circuits Syst.*, vol. CAS-23, no. 10, pp. 581–590, Oct. 1976.

[7] H. A. Haus and R. B. Adler, *Circuit Theory of Linear Noisy Networks*. New York: Wiley, 1959.

[8] J. Randa, "Noise characterization of multiport amplifiers," *IEEE Trans. Microw. Theory Tech.*, vol. 49, no. 10, pp. 1757–1763, Oct. 2001.

[9] L. Belostotski and J. W. Haslett, "A technique for differential noise figure measurement of differential LNAs," *IEEE Trans. Instrum. Meas.*, vol. 57, no. 7, pp. 1298–1303, Jul. 2008.

[10] E. G. Nielsen, "Behavior of noise figure in junction transistors," *Proc. IRE*, vol. 45, no. 7, pp. 957–963, Jul. 1957.

[11] R. J. Hawkins, "Limitations of Nielsen's and related noise equations applied to microwave bipolar transistors, and new expression for the frequency and current dependent noise figure," *Solid State Electron.*, vol. 20, no. 3, pp. 191–196, 1977.

[12] H. Hillbrand and P. H. Russer, "An efficient method for computer aided noise analysis of linear amplifier networks," *IEEE Trans. Circuits Syst.*, vol. CAS-23, no. 4, pp. 235–238, Apr. 1976.

[13] L. Moura, P. P. Monteiro, and I. Darwazeh, "Generalized noise analysis technique for four-port linear networks," *IEEE Trans. Circuits Syst. I, Reg. Papers*, vol. 52, no. 3, pp. 631–640, Mar. 2005.